

Recent Developments in Earthquake Hazards Studies

Walter D. Mooney and Susan M. White

Abstract In recent years, there has been great progress understanding the underlying causes of earthquakes, as well as forecasting their occurrence and preparing communities for their damaging effects. Plate tectonic theory explains the occurrence of earthquakes at discrete plate boundaries, such as subduction zones and transform faults, but diffuse plate boundaries are also common. Seismic hazards are distributed over a broad region within diffuse plate boundaries. Intraplate earthquakes occur in otherwise stable crust located far away from any plate boundary, and can cause great loss of life and property. These earthquakes cannot be explained by classical plate tectonics, and as such, are a topic of great scientific debate. Earthquake hazards are determined by a number of factors, among which the earthquake magnitude is only one factor. Other critical factors include population density, the potential for secondary hazards, such as fire, landslides and tsunamis, and the vulnerability of man-made structures to severe strong ground motion. In order to reduce earthquake hazards, engineers and scientists are taking advantage of new technologies to advance the fields of earthquake forecasting and mitigation. Seismicity is effectively monitored in many regions with regional networks, and world seismicity is monitored by the Global Seismic Network that consists of more than 150 high-quality, broadband seismic stations using satellite telemetry systems. Global Positioning Satellite (GPS) systems monitor crustal strain in tectonically active and intraplate regions. A relatively recent technology, Interferometric

Synthetic Aperture Radar (InSAR) uses radar waves emitted from satellites to map the Earth's surface at high (sub-cm) resolution. InSAR technology opens the door to continuous monitoring of crustal deformation within active plate boundaries. The U.S. Geological Survey (USGS), along with other partners, has created ShakeMap, an online notification system that provides near-real-time post-earthquake maps of ground shaking intensity. These maps are especially useful for the coordination of emergency response teams and for the improvement of building codes. Using a combination of these new technologies, with paleoseismology studies, we have steadily improved the science of earthquake *forecasting* whereby one estimates the probability that an earthquake will occur during a specified time interval. A very recent development is Earthquake Early Warning, a system that will provide earthquake information within seconds of the initial rupture of a fault. These systems will give the public some tens of seconds to prepare for imminent earthquake strong ground motion. Advances in earthquake science hold the promise of diminishing earthquake hazards on a global scale despite ever-increasing population growth.

Keywords Diffuse plate boundary · Earthquake · Global positioning system · Paleoseismic record · Seismic tremor

Introduction

In recent years, it has been suggested that the threat of earthquakes as a global natural hazard has decreased. Statistics published in 2002 by the United Nations

W.D. Mooney (✉)
USGS, Menlo Park, CA 94025, USA
e-mail: mooney@usgs.gov

indicated that there have been a decreasing number of fatalities (as a percentage of global population) resulting from earthquakes in recent decades (United Nations, 2002). A somewhat different perspective is provided when considering the effects of the 2004 Indian Ocean earthquake and tsunami, the 2005 Kashmir, Pakistan, and the 2008 Sichuan, China earthquakes. Together, these three events caused more than 400,000 deaths and left more than 10 million people homeless.

It is increasingly recognized that mega-cities throughout the world, especially those in developing countries, are highly vulnerable to major earthquakes. While the repeat time for some large earthquakes is several centuries or longer, many large cities in earthquake hazard zones across the globe are less than a century old and thus their built environment is untested in terms of their vulnerability to earthquakes (Bolt, 2006). Moreover, the occurrence of major earthquakes away from plate boundary zones in such locations as Bhuj, India (2001, $M = 7.6$) and the New Madrid Zone in Missouri (1811–1812, $M = 7-8$) serve as a reminder that earthquakes are a global hazard. Hence, urban centers with a high population density may expect increased fatalities from future earthquakes unless necessary precautions are taken.

There are reasons to believe that earthquake losses can be reduced. Research and the development of new technologies will allow for improved earthquake forecasting through an understanding of both past earthquakes and phenomenon such as stress transfer between active faults. However, earthquake forecasting will not reduce losses unless both developing and wealthier countries focus on mitigation strategies for earthquake hazards and strengthening their existing infrastructure through retrofitting and implementing building codes.

The Science of Earthquakes – Understanding the Hazard

Background

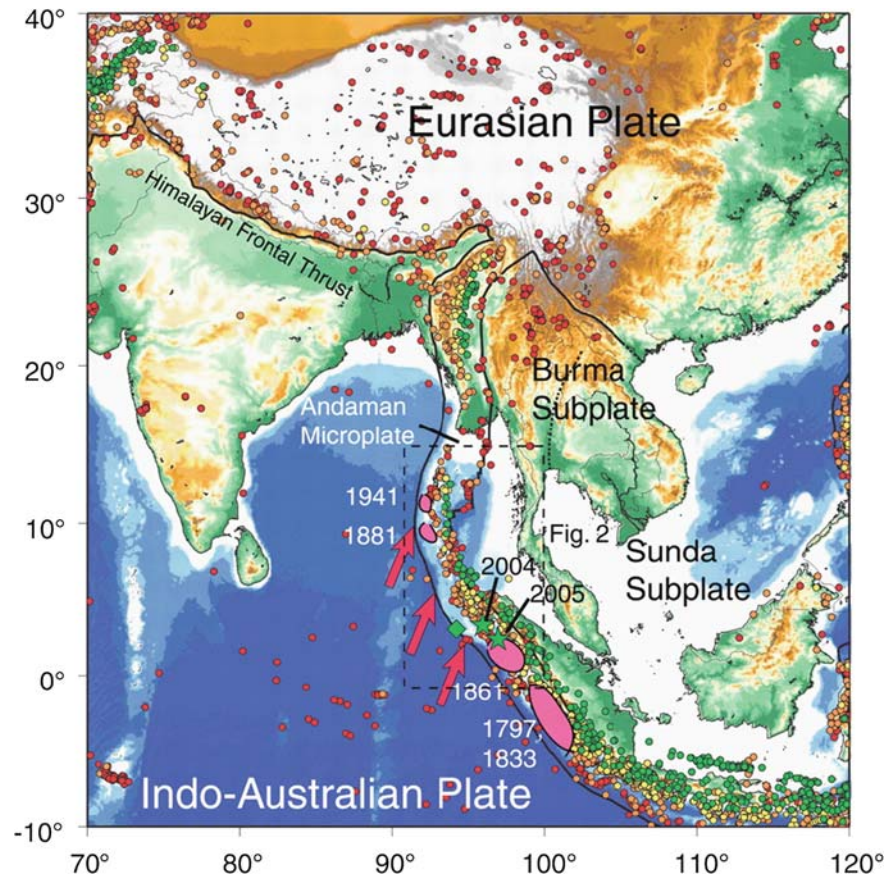
Earthquakes are a natural phenomenon that have been documented and studied since written records began. During the fourth century B.C. a prominent Indian sage

and family priest, Garga, theorized that earthquakes were caused by the sigh of the elephants that carry the Earth (Tagare, 2002). In the same century Aristotle suggested that earthquakes were caused by winds trapped in underground caves. The earthquake of 1755 that devastated Lisbon, Portugal, occurred on a major religious holiday and stirred much debate throughout Europe, thereby playing a role in The Enlightenment. Several recent earthquakes have attracted an international response and public policy discussion, as demonstrated by the response to the $M_w = 9.3$ December 26, 2004, Sumatra-Andaman Islands earthquake (Fig. 1) and the $M_w = 7.9$ Sichuan, China earthquake of May 12, 2008.

Our understanding of how and where earthquakes occur has improved significantly throughout history, most notably starting with the invention of the pen-and-paper seismograph in the 1880s. Studies of the great 1906 San Francisco earthquake played a major role in understanding the relation between earthquake ground motions and fault slip (Lawson, 1908; Reid, 1910). The advent of plate tectonics theory in the 1960s marked the greatest advancement in earthquake studies. The development of seismology, and the study of elastic waves propagating through solid and molten rock, revealed the presence of distinct layers now commonly recognized as the Earth's core, mantle, and crust. Our current theory of earthquake generation lies with the understanding that the upper, rigid outer shell of the crust and mantle, known as the lithosphere, is divided into numerous tectonic plates that continuously drift across the underlying, hot, partially molten asthenosphere. These tectonic plates meet one another at plate boundaries where they may collide, rift apart, or drag against each other, resulting in earthquakes.

The largest earthquakes occur at subduction zones where the oceanic lithosphere descends beneath the overriding continental lithosphere along what is called a megathrust fault. This follows from the fact that earthquake magnitude is proportional to the total area of the fault and the amount of slip. Whereas the Richter magnitude is familiar to the public, seismologists generally use the moment magnitude (M_w ; Bolt, 2006) which is a more accurate measure of earthquake size. It is not uncommon for subduction zones to experience 10–20 m of slip, values that are rare elsewhere. Likewise, the dimensions of the fault surface area for subduction zone earthquakes can easily

Fig. 1 Tectonic setting of Southeast Asia and the collision zone formed between the Eurasian and Indo-Australian plates. The dates of recent and historic earthquakes at the Indonesian/Andaman Islands subduction zone are shown. The $M_w = 9.2$ earthquake of 2004 generated a tsunami that devastated the coastline within this region



reach 1,000 km in length and 200–300 km in downdip extent. In contrast, continental strike-slip faults typically extend to a depth of only 15–30 km, and the longest mapped extent of a continental fault rupture is about 430 km (2001 Kunlun Shan, China; Xu et al., 2006). The larger area of subduction zone mega-thrust faults means that their earthquakes may have moment magnitudes in excess of $M_w = 9$, whereas continental earthquakes rarely exceed $M_w = 8.0$. In addition to megathrust earthquakes, subduction zones generate two additional types of earthquakes. Intraslab earthquakes occur to depths as great as 660 km and reach moment magnitude 8. Crustal earthquakes occur in the overriding plate due to stresses produced by the subduction process. Such crustal earthquakes are particularly hazardous due to their shallow depth and proximity to population centers. An example is the 1995 Kobe, Japan, earthquake that resulted in nearly 6,000 deaths.

One might expect that the larger subduction zone earthquakes would also be the deadliest. However,

for several reasons, this is not the case. In the past 100 years, 10 of the 14 most deadly earthquakes have occurred on continental faults. The level of hazard posed by continental earthquakes can be appreciated by comparing two recent large events. The $M_w = 7.9$ Peru subduction zone event of Aug. 16, 2007 caused 517 deaths. In contrast, the $M_w = 7.9$ Sichuan, China, event of May 12, 2008 caused more than 90,000 deaths. The critical factor is that continental faults may pass directly beneath the affected communities, whereas subduction megathrusts are largely offshore, and thus strong ground shaking is attenuated.

While damage from strong ground shaking may be greater for continental earthquakes, subduction zone earthquakes pose an additional hazard from tsunamis. Ground shaking from the $M_w = 9.3$ Sumatra-Andaman Islands earthquake of December 26, 2004, caused little damage, but the resulting tsunami claimed more than 230,000 lives throughout the Indian Ocean basin (Fig. 1).

Diffuse Plate Boundaries

Plate boundaries are typically conceived of as narrow contact regions between tectonic plates that can be represented as a single fault on a map. Examples of well-defined plate boundaries include the great subduction zones that circle the Pacific Ocean or the Anatolian fault in northern Turkey. Classical plate tectonics recognizes the presence of ten plates covering the Earth's surface, but this number has grown with the identification of several microplates such as the Juan de Fuca or Borneo plates. In fact, there is no consensus on the precise location of some plate boundaries as the term is conceived in classical plate tectonics. For example, the southern boundary between the Caribbean and South American plates is poorly defined, as is the boundary between the South American, Antarctic, and Scotian plates, the boundary between the Somalia and Nubia plates, and the boundary between Australian and Pacific plates (Fig. 2).

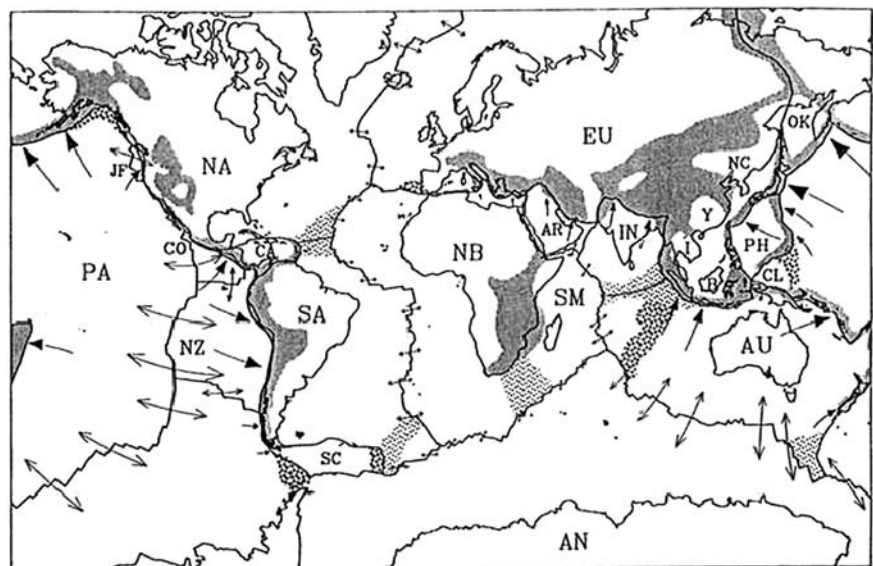
Thus, the width of a plate boundary can range from several hundred meters to several thousand kilometers. Wide plate boundaries occur where the crust and mantle lithosphere are actively deforming, and we refer to these regions as diffuse plate boundaries. It is estimated that approximately 15% of the Earth's surface is composed of these actively deforming regions (Gordon, 1995; Fig. 2). Classical tectonic theory is not sufficient to describe the kinematics that gov-

ern large scale movement at diffuse plate boundaries (Gordon and Stein, 1992). There may be hundreds of individual fault-bounded blocks separating one rigid plate from another across such wide boundary zones. Furthermore, the contact point between diffuse plate boundaries and plate interiors may also be gradual and indistinct (Gordon, 1995). Earthquakes, which are concentrated at plate boundaries, are geographically distributed throughout the diffuse plate boundary thereby spreading seismic hazards over a much broader region.

The Earthquake Cycle

The elastic rebound theory is the classical approach to explain how strain is distributed during the earthquake cycle and the mechanical process that takes place between one earthquake and the next on a particular fault (Reid, 1910). As tectonic plates gradually move past one another, there are some portions along the plate boundary where the plates are locked. At these locked areas of contact, strain accumulates and slow internal deformation takes place until the friction on the fault is exceeded and the plates suddenly slip. Global Positioning Satellite (GPS) data provide a means of monitoring crustal strain. Over a sufficiently long period of time the rate of strain energy

Fig. 2 Map showing idealized narrow plate boundaries, measured plate velocities, and regions of deforming lithosphere (light and dark shading), which are regarded as diffuse plate boundaries. Plate velocities are shown by arrows; their length indicates the magnitude of displacement expected in a period of 25 millions years (after Gordon, 1995)



accumulation must balance the seismic strain release in the form of earthquakes. After an earthquake nucleates at the hypocenter, fault rupture propagates along the fault at a velocity near 3 km/s and radiates elastic energy off the fault surface. Assuming a constant stress drop, the larger the rupture area and amount of fault slip, the greater the amount of seismic energy that is released, and the more damaging is the strong ground motion. We note that some continental earthquakes, such as the $M_w = 7.6$ Bhuj, India, event were high-stress drop events, and therefore had a smaller fault area in comparison with other earthquakes with the same moment magnitude.

A complete description of the earthquake cycle incorporates interseismic (i.e., the time period between large seismic events) and postseismic deformation in addition to the coseismic deformation that takes place during an earthquake (Tse and Rice, 1986; Fig. 3). In these models of the earthquake cycle, slow, creeping displacement occurs in the viscous lower crust and lithosphere prior to the earthquake. This interseismic viscous creep can take place over a period of centuries for faults with long recurrence intervals. Eventually, the colder upper crust must “catch up” and release accumulated strain in a sudden coseismic displacement (an earthquake). Postseismic deformation is typically

in the form of viscous creep and occurs over a period of days to weeks following an earthquake. The sum of all types of displacement over the earthquake cycle is known as the earthquake’s total slip budget. Global Positioning Satellite (GPS) measurements, discussed in a later section, are able to track the progress of the interseismic, coseismic, and postseismic phases of the earthquake cycle along the Parkfield segment of the San Andreas Fault (Bakun et al., 2005; Murray and Langbein, 2006; Johanson et al., 2006).

In general, earthquakes in continental regions occur in the upper and middle crust (< 25 km depth). Earthquakes in the deeper continental crust (> 25 km depth) are rare, but some deep events are reported in old, cold crust such as the Indian craton (Raphael and Bodin, 2002; Kayal et al., 2002; Mishra and Zhao, 2003). The strength of the lithosphere depends on several factors, including pressure and temperature. The temperature in the crust typically increases by 10 to 30°C/km. The depth of continental earthquakes tells us that the upper and middle crust is in the brittle regime of failure, whereas the lower crust and mantle lithosphere undergoes creeping (ductile) deformation. Frictional strength increases linearly with pressure (depth) and ductile strength decreases exponentially with temperature. Combining both the ductile and brittle relations

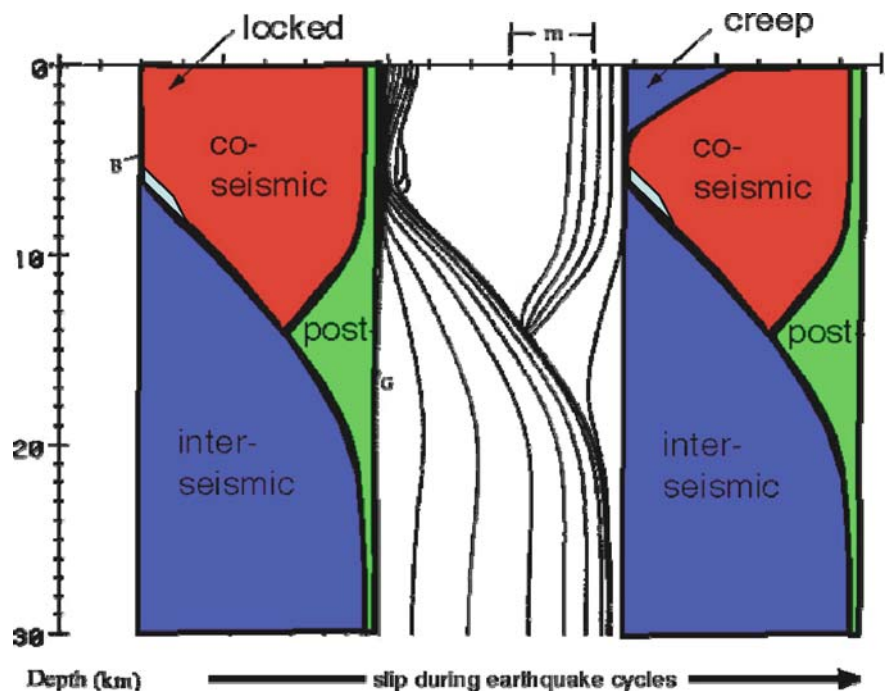
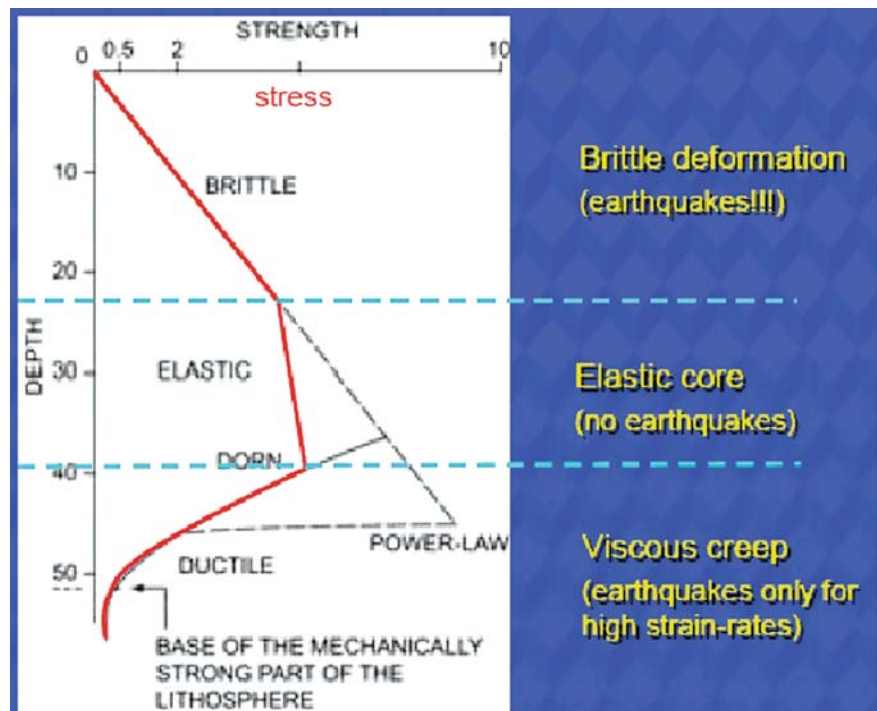


Fig. 3 The earthquake cycle, from the interseismic period, with lower crustal creep (blue on left side), co-seismic slip that occurs during fault rupture (red), and post-seismic relaxation (green). In this model the locked portion of the upper crust is loaded from below by the creeping middle and lower crust

Fig. 4 Strength (stress)-depth curve for the crust and elastic lithosphere. Stress increases in the brittle crust until a mid-crustal transition zone with reduced strength is reached. At greater depth, in the ductile mantle, viscous creep occurs. Earthquakes occur primarily in the brittle upper crust (Source: Cloetingh, 1982)



yields an overall rheological strength profile for the lithosphere as a function of depth (Fig. 4). Shallow crustal earthquakes are therefore due to brittle deformation in the colder upper crust, whereas the weak, ductile lower crust and mantle lithosphere undergoes steady creep.

An important aspect of the earthquake cycle is the recurrence interval, the statistical average time period between large earthquakes along a particular segment of fault line. The recurrence interval for an earthquake of a given magnitude, say $M_w = 7$, is dependent on the strain rate. Since a $M_w = 7$ earthquake has about 4 m of slip, a low strain rate of 4 mm/year (as might occur within a diffuse plate boundary, or in an intraplate environment) will require about 1,000 years to accumulate 4 m of strain. Regions with a high strain rate of 40 mm/year, as found on the Main Boundary Fault of the Indian Himalayas, will accumulate 4 m of strain in just 100 years if these faults are fully locked.

Knowledge of the present strain rate and the recurrence interval (with standard deviation) on a fault makes it possible to estimate the probability of an earthquake occurring on a particular fault within a

specific time window, such as 10 years. Such probabilistic estimates are very useful in planning seismic mitigation. Although earthquake prediction may not be feasible in the foreseeable future, earthquake *forecasting*, based on recurrence intervals, has become more sophisticated and reliable in recent years.

Earthquake Triggering: Natural and Man-Made

The stresses in the Earth's crust gradually increase due to global tectonic processes except when a fault is creeping. It is not surprising, then that many faults are already near the point of failure; such faults are referred to as critically stressed faults (Zoback and Townend, 2001). Only a relatively small increase in stress will cause the fault to fail, causing an earthquake. All that is required is an extra "push" (stress increase) on a favorably oriented, critically stressed fault. Such earthquakes are called triggered earthquakes.

There are two primary types of triggered earthquakes, those induced by man-made stress increases and those induced by other earthquakes. Man-made stress increases include the filling of water reservoirs, mining activities and nuclear weapon testing (Simpson, 1986). The 1967 $M = 6.5$ earthquake at Koa reservoir, India, resulted in 200 deaths and 1,500 injuries (Gupta et al., 1972). This earthquake is generally considered to be a triggered earthquake.

Earthquakes cause static stress changes in the neighboring crust. The regional static Coulomb stress change due to an earthquake can be calculated if the fault geometry and slip distribution is known (King et al., 1994; Freed, 2005). These regional stress changes following a large earthquake can explain many seismic observations including both triggered earthquakes and seismic quiescence in regions that previously were seismically active (Stein et al., 1997; Stein, 1999).

Stress changes in the crust following an earthquake may be permanent (static) or transient and dynamic. As an example of dynamic triggering, it has been suggested that high-amplitude surface waves from the great ($M = 9.3$) Indonesian earthquake of December 2004 may have triggered micro-earthquakes as far away as Alaska (West et al., 2005). Theoretical modeling has suggested that dynamic stress is only able to cause “nearly instantaneous failures” on secondary faults, whereas there are often long delays before an earthquake occurs due to static stress changes (Belardinelli et al., 2000). However, predicting exactly how and when earthquake triggering will occur has not been possible since all earthquakes affect a very large, complex system of interacting faults across the Earth’s crust.

Intraplate Earthquakes

The previous discussion has focused on earthquakes that occur either at well-defined plate boundaries, such as subduction zones, or within diffuse plate boundaries, such as the Tibetan Plateau. Earthquakes may also occur well away from a plate boundary, either in the ocean, typically on a transform fault, or in so-called stable continental crust. Such events are known as intraplate earthquakes (Fig. 5) and can cause sig-

nificant loss of life when they occur near population centers. Some intraplate earthquakes at northern latitudes are caused by crustal unloading due to deglaciation. However, the ultimate cause of most intraplate earthquakes is the compressional state of stress of the Earth’s crust due to the mid-ocean ridge push and asthenospheric viscous drag resistance to plate motions (Zoback and Zoback, 1980; Zoback, 1992). This stress is an effect of the gravitational potential energy of the oceanic ridges’ elevated topography. The magnitude of this potential energy can be easily appreciated when one considers the towering heights of the Himalayas and Tibetan Plateau, which are the products of ridge push from the Indian Ocean ridge. Compression forces create critically stressed faults within plate interiors (Zoback and Townend, 2001), and a small increase in stress may result in an earthquake. The mechanism that localizes stress perturbations and causes intraplate earthquakes in some regions, but not others, is not well understood.

The strain rate in the ductile lower crust of intraplate regions may be expressed as (Goetze, 1978; Brace and Kohlstedt, 1980):

$$\text{Strain rate } (\dot{\epsilon}) = A \exp(-Q/RT)(S_1 - S_3)^n \quad (1)$$

where:

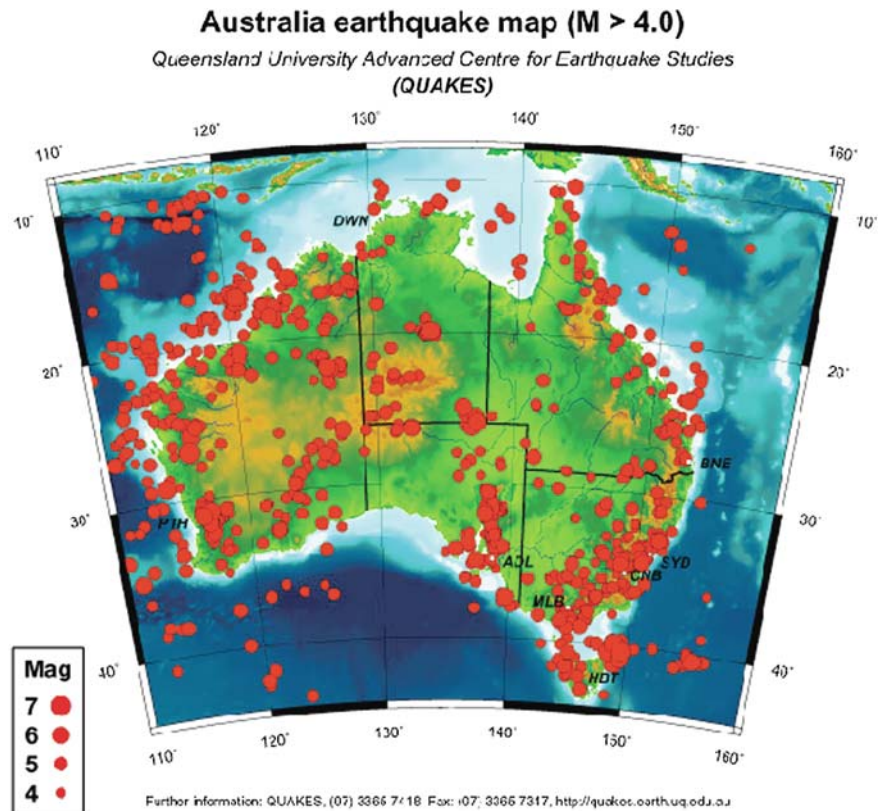
A is the flow parameter; Q is the activation energy; R is the gas constant; T is absolute temperature, and n is the stress exponent

S_1 is the maximum horizontal stress, and S_3 is the minimum horizontal stress.

Equation (1) implies that the strain rate will be at a maximum when the two horizontal stresses are at a maximum difference. The equation also implies that the strain rate will be higher for warmer thermal regimes (higher geotherm). These two implications may be used to infer that: (1) faster moving continental plates, such as India and Australia, will have higher strain rates due to the horizontal driving forces that move these plates; and (2) continental plates with thinner lithosphere will have high strain rates due to higher crustal temperatures (higher geotherm). Both of these inferences appear to be true for the Indian and Australian continental plates, which both have relatively high rates of intraplate seismicity (Fig. 5).

Continental intraplate earthquakes are widely distributed and are often associated with continental

Fig. 5 Seismicity of Australia and its continental margin. Continental earthquakes in Australia are abundant, and all are intraplate earthquakes. The origin of such earthquakes that occur away from plate boundaries is a subject of considerable scientific debate



margins and interior rifts (Fig. 5). In 1811 and 1812, a sequence of three large ($M_w \geq 7$) intraplate earthquakes occurred in New Madrid, Missouri, central USA. As summarized in Schulte and Mooney (2005), the New Madrid region is an example of intraplate seismicity associated with a paleo-rift, a correlation that has been found on a global scale in several studies (Sbar and Sykes, 1973; Sykes, 1978; Hinze et al., 1988; Johnston and Kanter, 1990; Johnston et al., 1994; Gangopadhyay and Talwani, 2003). The New Madrid earthquakes of the nineteenth century caused hundreds of casualties and were felt over an area of more than 120,000 square km. By comparison, the great 1906 ($M = 7.8$) earthquake of San Francisco was only felt over an area of 15,000 square km. In the eastern U.S., which is widely regarded as having a relatively low seismic hazard, a significant $M_w = 7.0$ to 7.3 earthquake struck Charleston, S.C., in 1886, and a large earthquake occurred off the coast of Cape Code in 1755 (the same year as the great Lisbon, Portugal, earthquake). The estimated recurrence interval for such events is estimated to be 400 years (Frankel et al., 1996).

In January 2001, a $M_w = 7.7$ earthquake occurred in Bhuj, western India, on a block of otherwise stable continental crust. The event caused more than 18,000 casualties, destroyed thousands of houses and critical infrastructure, and caused large ground motion more than 300 km away from the epicenter, or over a 260,000 square km region. It is evident that seismic waves emanating from earthquakes in older and colder crystalline continental crust will propagate farther, causing severe ground shaking and damage over a larger radius than those earthquakes emanating from the young, warm crust at plate boundaries. Although intraplate earthquakes contribute no more than 10% of the global released seismic energy, their widespread reach and unknown mechanism make them a cause for concern among seismologists (Bolt, 2006).

As discussed in Schulte and Mooney (2005), models that have been suggested to explain the occurrence of seismicity within continental interiors include localized stress concentration around igneous intrusions (Campbell, 1978), intersecting faults (Talwani, 1988, 1999) and ductile shear zones in the lower crust (Zoback, 1983). Fluids still present in the lower crust

of ancient rift zones (Vinnik, 1989), a weak zone in the lower crust (Kenner and Segall, 2000) and stress perturbation resulting from buried rift pillows (Zoback and Richardson, 1996) have also been suggested. Liu and Zoback (1997) proposed the hypothesis that seismicity is related to elevated temperatures at depth. In their model, plate-driving forces are largely supported by the strength of the (seismogenic) upper crust; the lower crust is weakened as a result of higher temperatures. Regions with a higher geothermal gradient will have a shallower brittle-ductile transition and thus the cumulative strength of the lithosphere will be lower. Saying “generally similar” model is presented by Long (1988) who suggested that intraplate seismicity is a transient phenomenon arising from a perturbation in crustal strength as a result of a disturbance in the hydraulic or thermal properties of the lower crust. Other models call for a perturbation of the regional stress field by forces associated with lithospheric flexure after deglaciation (Stein et al., 1979; Quinlan, 1984; Grollmund and Zoback, 2001), gravitational forces at structural boundaries (Goodacre and Hasegawa, 1980; Chandrasekhar and Mishra, 2002) or sediment loading (Talwani and Rajendran, 1991). The recurrence interval for intraplate seismic zones are currently debated, with estimates ranging from relatively short (200–300 year) intervals to much longer (500–2,000 year) intervals. However, we note that the shorter recurrence intervals for major earthquakes do not readily conform to the statistics inferred from the rate of microearthquake activity (Mandal and Rastogi, 2005) nor with low (1 mm/year or less) intraplate deformation rates determined from GPS data (Calais et al., 2006).

According to Schulte and Mooney (2005), many of the models for Stable Continental Region (SCR) seismicity listed above require features that are often found in ancient rifts: numerous large faults and intrusions, an anomalous crustal structure compared with the surrounding crust and possible remnant crustal fluids. However, SCR seismicity is not unique to rift zones. In their study of intraplate seismicity, Schulte and Mooney (2005) find that: (1) 27% of all events occur within continental rifts; (2) 25% occur at rifted continental margins; (3) 36% are within non-rifted crust; and (4) 12% remain uncertain in terms of tectonic setting. The largest events ($M_w \geq 7.0$) have occurred predominantly within rifts (50%) and continental margins (48%).

Transient Aseismic Slip and Subduction Zone Seismic Tremor

Large mega-thrust events and shallow crustal earthquakes are not the only kinds of seismic events that occur at subduction zones. The recent discovery of transient aseismic slip (detected with GPS data) and seismic tremor at subduction zones suggests that the physics of faults involves an even more complicated and subtle process than previously imagined. In the last decade, observations of this slow, aseismic slip and periodic seismic tremor at many subduction zones have shown that there are alternative ways for faults to release stress than the sudden slip of an earthquake (Hirose, 1999; Rogers and Dragert, 2003). Transient aseismic slip tends to occur near the base of the locked zone on a subduction megathrust. It is unknown why certain subduction zones display transient slip and others do not. It has been hypothesized that the trigger of transient aseismic slip and seismic tremor may be pore fluid migration producing a reduction of fault-normal stress accompanied by seismic tremor within the fluid conduits (Melbourne and Webb, 2003). Aseismic slip can be quite significant and may release the equivalent of a $M_w = 7$ earthquake (Kostoglodov et al., 2003). In the Cascadia subduction zone in western North America, the aseismic slip lasts 1–2 weeks with a recurrence period of 14 months, while in the Bungo Channel of Japan, the slip lasts some 300 days with a recurrence period of 6 years (Hirose, 1999), and in Guerrero, southern Mexico, one large “silent earthquake” lasted 6–7 months (Lowry et al., 2001). Dragert et al. (2001) suggest that aseismic deep-slip events could play a key role in the cumulative stress loading and the eventual failure of shallow seismogenic zones. However, a robust connection between great earthquakes and aseismic slip events has not been made. Rubinstein et al. (this volume) provides additional discussion of transient aseismic slip and seismic tremor.

The Paleoseismic Record

Paleoseismology permits the reconstruction of the earthquake history of an area using geologic evidence of faulting and/or liquefaction in combination with radiocarbon dating (Fig. 6). This field has expanded greatly in recent years with important new



Fig. 6 *Top*: Paleoseismic expedition. Geologists are looking for evidence of faulted layers of sediments and rock, injections of liquefied sand (sand blows), and evidence for abruptly raised or lowered shorelines. *Bottom*: Buried peaty soil in British

Columbia, the remains of a marsh that subsided 1.5 m during the 1700 Cascadia mega-thrust earthquake. The lighter color sand layer was then deposited by a tsunami that was caused by the earthquake

results obtained in Japan, New Zealand, China, Turkey, North America and the Mediterranean. Paleoseismic results show that earthquake recurrence intervals can range from about 20 years to more than 2,000 years.

The 1897 Great Assam (India) earthquake is the strongest instrumentally recorded intraplate earthquake, with an estimated $M_w = 8.7$. Mohindra and Bagati (1996) report paleoearthquakes in this region (the Shillong Plateau) dated at 1450–1650 AD, 700–1050 AD, and predating 600 AD. Together with the 1897 event, these data suggest a recurrence interval for this intraplate setting of 400–600 years. In northwestern India, a $M_w = 7.6$ earthquake occurred in 2001 in Gujarat (Bhuj), India, and was preceded by a similar strong event some 150 km to the NW in 1801. Paleoseismic investigations and evidence from ancient temples indicate that no large earthquakes have occurred in this region since the ninth century AD. Thus, the faults in this region appear to have recurrence intervals greater than 1,000 years.

As previously discussed, the New Madrid seismic zone of the central United States experienced three earthquakes of M_w greater than $M_w = 7.5$ in 1811–1812. Paleoliquifaction studies have determined similar large historic events at about 1450 AD, 900 AD 300 AD and 2350 BC (each date has an uncertainty of about 150 years; Tuttle et al., 2005). These results indicate a recurrence interval of about 500 years, which is about the same value as estimated for the 1897 Great Assam earthquake. However, these short recurrence intervals are enigmatic in view of the low regional strain rates measured with GPS data (Calais et al., 2006).

Paleoseismic techniques have also been applied to subduction zone settings. Seismic hazards in the Pacific Northwest are due to the subduction of the Juan de Fuca plate beneath the North American plate (the Cascadian subduction zone). This subduction is also responsible for the volcanic activity throughout the Pacific Northwest including the eruption of Mount St. Helens in 1980. A significant portion of the plate boundary between the Juan de Fuca and North America plates is locked (Savage et al., 1981; Dragert and Hyndman, 1995) raising the possibility that the Cascadian subduction can produce a megathrust earthquake ($M_w > 8.0$) that could rupture along its entire 1,100 km length and generate a tsunami comparable to the 2004 Indian Ocean tsunami. Indeed, by using paleoseismol-

ogy, one such earthquake (and the resulting tsunami) was recently determined to have occurred in 1700, causing significant devastation to harbors in Japan and no doubt throughout many other coastal communities in the Pacific region (Nelson et al., 1995; Satake and Atwater, 2007).

Lessons from the Earthquake Record

A Survey of Earthquake Hazards

The primary hazardous effect of an earthquake is strong ground motion, which is measured in terms of acceleration and velocity. The strong ground motions of concern to civil engineers are usually those occurring near to the earthquake source, typically from 1 km to about 25 km, depending on the earthquake magnitude and regional seismic attenuation relations. Ground motions near the earthquake source are important because these motions are strong enough to endanger the built environment. Near-field ground motion data are also the most valuable data concerning the detailed properties of the source mechanism of the earthquake, i.e., geometry of the fault plane, the amount of slip as a function of space and time, and the rupture velocity. Each of these factors will affect the energy that is radiated during the rupture process. In order to design more earthquake resistant structures, a major effort has been made to model strong ground motion data including the duration, frequency content and fault radiation patterns. Earthquake strong ground motion data are thus of mutual interest to seismologists and engineers. In recent years it has been shown that most large (fault dimension greater than 100 km) earthquakes are usually complex multiple events (Kanamori, 2005), often making it difficult to model short period (less than 1 sec) ground motions. Progress in modeling near-field strong motion data has recently advanced due to the installation of significantly denser strong motion recording networks.

In addition to damaging strong ground motion, earthquakes may generate even more destructive secondary effects, such as liquefaction, landslides, tsunamis and fires. There are many examples of such effects, including April 18, 1906, $M_w = 7.8$ Great San Francisco earthquake that produced powerful ground



Fig. 7 Photographs taken after the 1906 Great San Francisco earthquake and fire. *Left:* damage to houses on the east side of Howard Street near Seventeenth Street. *Right:* The remains of the

Hibernia bank on Market Street. The fire caused more destruction than the ground shaking of the earthquake

shaking that affected all of coastal northern California (Freed et al., 2007). Property damage amounted to \$524 million and the number of fatalities reached 3,000 (Fig. 7). Broken water mains prevented firefighters from battling the numerous fires that appeared all over the city. In this case, the fires that raged in the city for three days caused more damage and loss of life than the earthquake (Cutcliffe, 2000). This earthquake and the 1934 Long Beach, California, event led to the adoption of better building codes in the State of California.

The Great Kanto (Tokyo region, Japan) earthquake of 1923 is another example of an earthquake with deadly secondary effects. This event resulted in more than 100,000 deaths and two million homeless, largely due to fires. The greater Tokyo region is home to about a quarter of the Japanese population of 130 million people. Paleoseismic evidence indicates that there have been seventeen $M_w \geq 8$ earthquakes in the Tokyo region in the past 7,000 years (Shishikura, 2003). This implies a long-term average recurrence interval of about 400 years for large events, with the last two $M_w = 8$ events having occurred in 1703 and 1923. The probability of a repeat of the 1923 Great

Kanto earthquake is estimated to be just 0.5% in the next 30 years (Stein et al., 2006). However, $M_w = 7.3$ earthquakes occur more frequently than every 400 years, the last such event having occurred in 1855 (the Ansei-Edo event). According to the Japanese government, a $M_w = 7.3$ earthquake beneath Tokyo, similar to the 1855 event, could cause more than 11,000 deaths and destroy 240,000 or more homes. The estimates losses would amount to US\$1 trillion. Stein et al. (2006) estimate that an event with a similar magnitude and location as the 1855 event has a twenty percent likelihood within a 30 year period.

The Japanese population was exposed to a dangerous secondary hazard on July 16, 2007, when a $M_w = 6.6$ earthquake occurred in close proximity to Kashiwazaki-Kariwa (KKNPP), the third largest nuclear power plant in the world (Fig. 8). Strong ground shaking caused a minor fire to break out, knocked over 100 barrels of low-level nuclear waste and required the power plant to be shut down. The plant, owned by Tokyo Electric Power Company (TEPCO), has seven boiling water reactors sitting on approximately 4.2 km² of land, and is home to seven of Japan's fifty five nuclear reactors, and produces



Fig. 8 The Kashiwazaki-Kariwa nuclear power plant (KKNPP), located about 10–20 km from the epicenter in the Niigata prefecture. This power plant was shut down after the July 16, 2007, earthquake caused damage to the plant

over thirty percent of the nation's power. All Japanese nuclear facilities have been engineered to withstand earthquakes of up to $M_w = 6.5$. In this instance, implementation of earthquake building codes in Japan's nuclear facilities almost certainly saved lives.

- Tsunamis are another secondary effect of earthquakes. In one well known case, the $M_w = 9.2$ earthquake that struck the coast of Sumatra, Indonesia, in December of 2004 triggered an Indian Ocean tsunami that devastated several countries separated by more than 4,000 miles, from Southeast Asia to Africa. The tsunami death toll exceeded 230,000 and led to the displacement of millions of people.
- A $M_w = 7.9$ earthquake struck eastern Sichuan, China, on May 12, 2008, and resulted in the death of some 89,000 people and left over a million homeless. This earthquake occurred within the Longmen Shan region which is located at the bound-

ary between the high topography of the Tibetan Plateau to the west and the relatively stable Sichuan Basin to the east (Fig. 9; Burchfiel et al., 1995). The ground shaking was felt over much of central, eastern, and southern China (Fig. 9). The earthquake led to numerous landslides that buried villages and complicated rescue efforts by blocking transportation routes. Medical supplies, water, and food may not reach isolated communities affected by the disaster and the inability to distribute critical supplies may dramatically increase the casualties.

Earthquake Engineering and Building Codes

The design of buildings to sustain earthquake strong ground motions is a critical step in reducing the loss

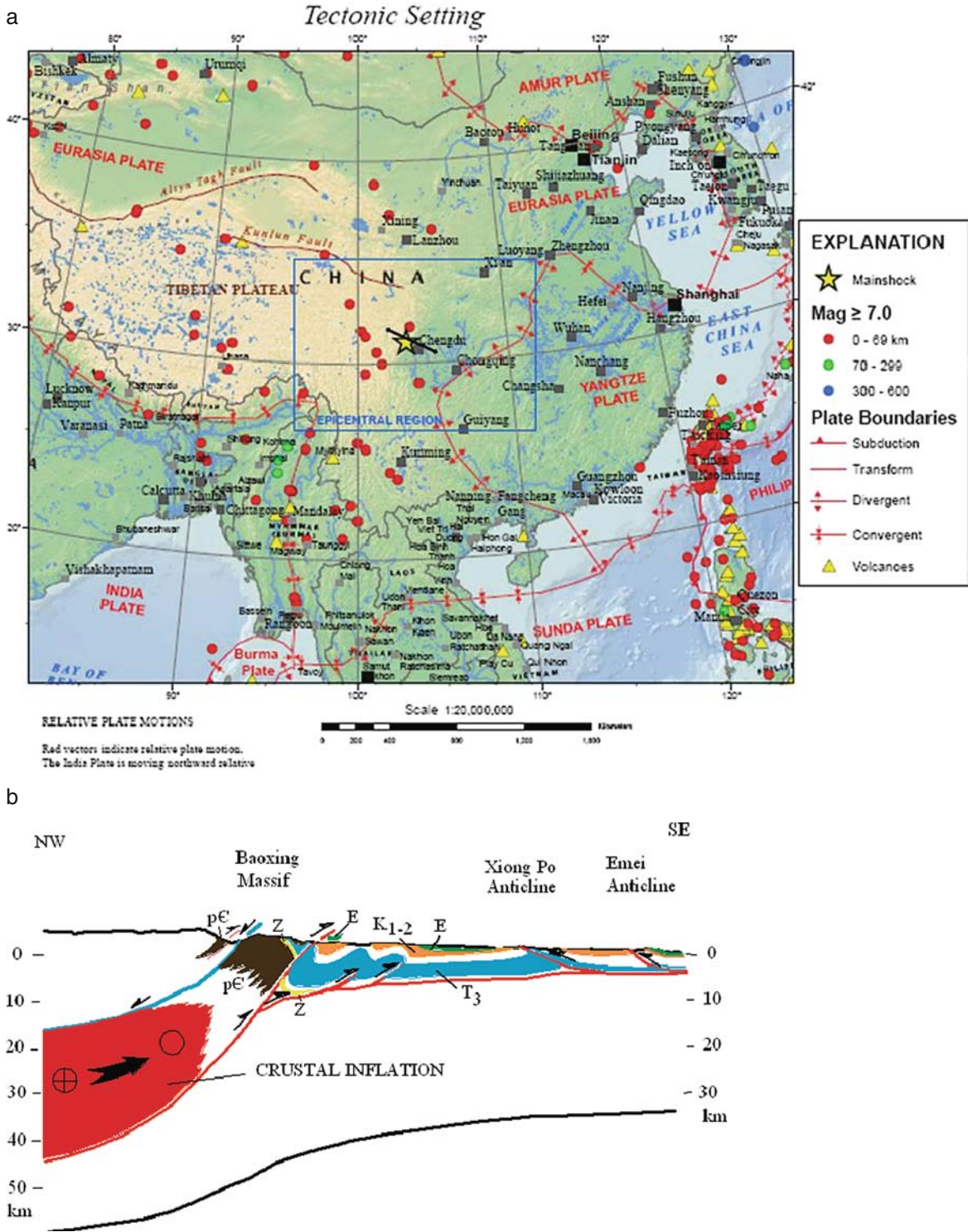


Fig. 9 A: Location map of China and neighboring countries. Star in center of map marks the location of the Mw = 7.9 Wenchuan (Sichuan Province) earthquake. The epicenter is on the eastern flank of the Tibetan Plateau. Black line near star

marks the location of cross-section in part B: Crustal cross section at the hypocentral location of the Wenchuan, China, earthquake. The thicker crust of the Tibetan Plateau is being thrust eastward over the neighboring Sichuan basin

Fig. 10 Rescue workers and local residents search for survivors in the rubble following the August 15, 2007, $M_w = 8.0$ Pisco, Peru earthquake. Many of the deaths and injuries occurred in homes constructed with highly vulnerable adobe bricks



of life. The importance of building codes was highlighted by the August 15, 2007, earthquake in Pisco, Peru (USGS, 2007). Peru is a country where traditional and modern building designs are found in close proximity. Adobe buildings account for 65% of all buildings in rural areas and nearly 35% of all buildings in urban areas. Adobe bricks are indigenous, sun-dried building materials consisting of sand (50–70%), clay (15–30%), and silt (0–30%), that are often mixed with a binding material, such as straw. Adobe brick walls are highly vulnerable to collapse when subjected to severe ground shaking. When the $M_w = 7.9$ Pisco earthquake struck, many of the adobe houses in Pisco and Ica collapsed, whereas the modern reinforced concrete buildings were only superficially damaged (Fig. 10). There were more than 500 fatalities due to the Pisco earthquake, and an estimated 58,000 homes (80% within the city of Pisco) were destroyed, leaving more than 250,000 people without shelter (Fig. 10).

Disaster struck Iran in 2003, when a $M_w = 6.6$ earthquake ruptured along the Bam Fault in central Iran. The earthquake caused 43,000 fatalities, most of these due to building collapse (Eshghi and Zaré, 2004). Like Peru, the Bam area of Iran also utilizes traditional housing constructed from adobe. The tectonic setting of the Bam, Iran, earthquake is crustal compression and reverse faulting, as confirmed by earthquake focal

mechanisms and analogue stress models of this continental collision zone (Fig. 11; Eshghi and Zaré, 2004; Sokoutis et al., 2003).

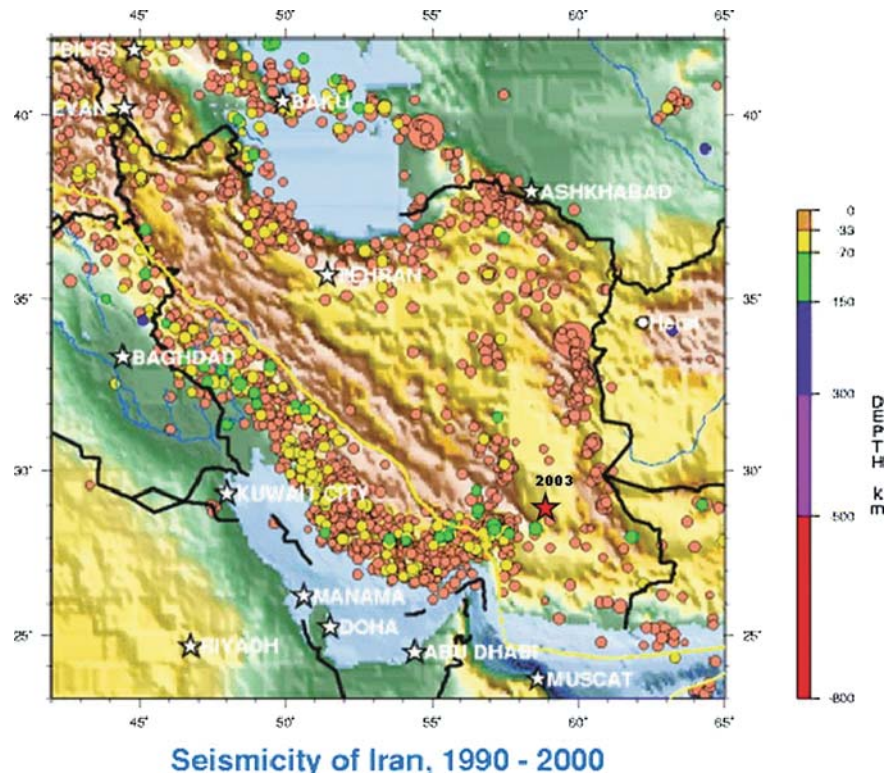
It is not always the case that traditional structures are weaker than modern designs. In the 2005 $M_w = 7.6$ Kashmir earthquake in Pakistan, western-style construction such as concrete block and brick masonry structures suffered more intense damage than the traditional timber-brick masonry typically used in this region (Naseem et al., 2005). In this case, buildings constructed using traditional styles and timber materials responded much better to ground shaking than all other building types. Traditional wood-framed buildings in Indonesia also perform much better than modern brick or unreinforced concrete building. A comparison of the 2005 Kashmir earthquake to the Pisco and Bam earthquakes indicates the importance of creating a building code appropriate for each specific region.

Future Directions in Earthquake Science

Enhanced Seismic Monitoring

Seismic monitoring systems have undergone tremendous growth during the past twenty-five years. The Global Seismic Network (GSN) was initiated by the

Fig. 11 Seismicity map of Iran, with location of the $M_w = 6.6$ Bam earthquake (red star) of 2003 that caused some 43,000 fatalities. The recurrence interval for large earthquakes in this region is estimated to be more than 1,000 years. However, even regions with long recurrence intervals may be highly vulnerable to earthquake disasters



Incorporated Research Institutions for Seismology (IRIS) and now has more than 150 high-quality, broadband seismic stations (Fig. 12). This system is operated in collaboration with the US Geological Survey and the University of California-San Diego. Some 75% of these stations are available in realtime using satellite telemetry systems.

Many national seismographic systems have also been upgraded. The disastrous 1995 Kobe earthquake in Japan led to major upgrades in the seismic monitoring systems in that country. These include a high-sensitivity seismic array with 698 stations, a broadband array with 74 stations (F-net) called Hi-net and a strong-motion network with 1,043 accelerometers. The high-sensitivity array can rapidly and accurately locate earthquakes; the broadband array provides data on the earthquake source; and the strong motion array provides earthquake engineering data (as well as information about the source). A similar program of network upgrades has been completed in Taiwan. In mainland China, there are more than two thousand short-period seismographs, two hundred broadband stations and more than four hundred accelerometers. In Europe,

a federation of national seismic systems, and international data collection program (e.g., ORFEUS and GEOSCOPE) provide abundant realtime data. In the United States, the Advanced National Seismic System (ANSS) is a comprehensive system that provides realtime seismic data from seismic sensors located in the free field and in buildings. Similar to other national networks, instrumentation includes a network of broadband sensors, accelerometers and high-gain seismic stations. The total number of sensors exceeds 7,000 in number, and the system automatically broadcasts information when a significant event occurs. Significant network upgrades have taken place in Mexico, Thailand, and Malaysia.

Global Positioning Systems (GPS)

Global Positioning Satellite (GPS) technology can detect minute motions of the Earth's crust that increase the stress on active faults and eventually leads to earthquakes (Segall and Davis, 1997). This technology

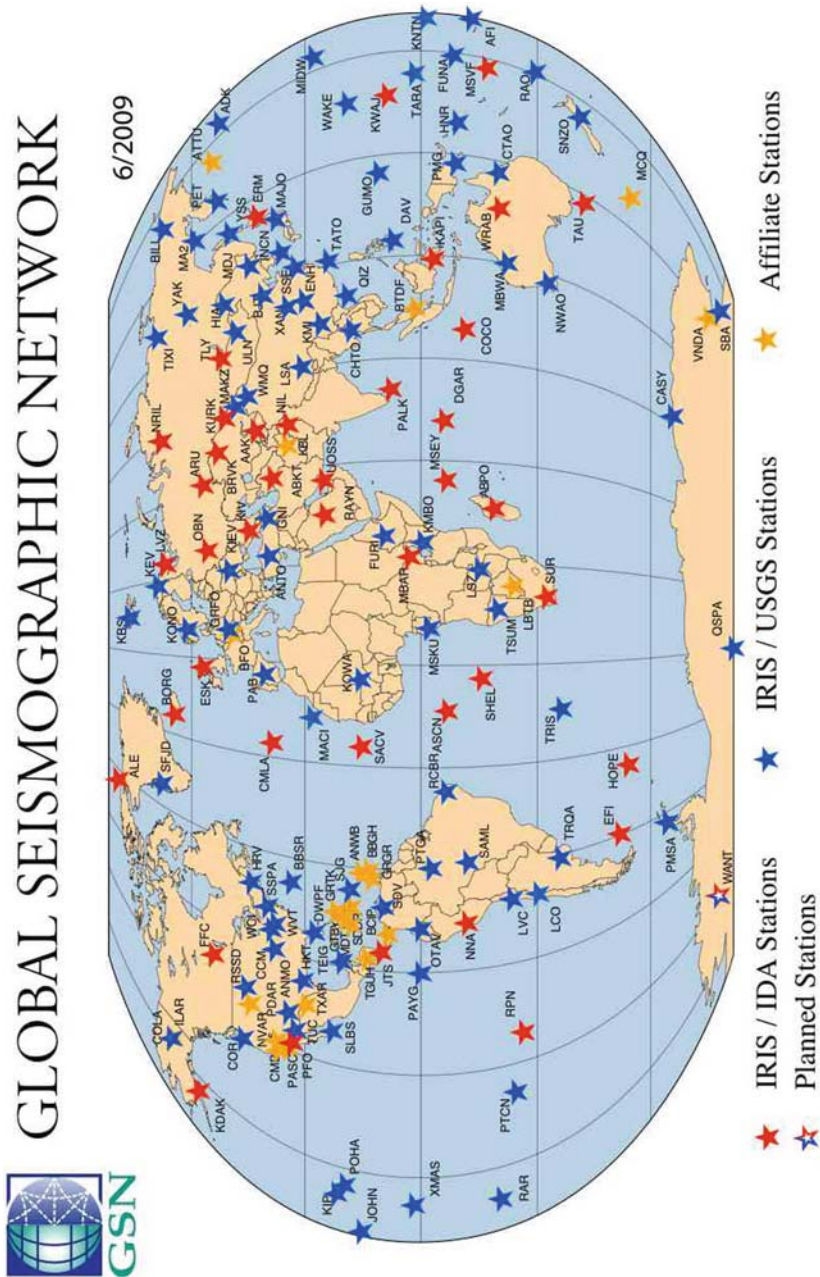


Fig. 12 Map of station locations of the Global Seismographic Network that monitors worldwide seismicity. All stations are located on continents and oceanic islands. Further sea-bottom stations are planned, but face technical challenges

provides an excellent picture of how slip (or ground displacement) can accumulate on faults throughout the earthquake cycle (e.g., Bakun et al., 2005). Satellites deployed across the globe emit precisely timed radio signals to tracking stations on the ground that record both gradual, aseismic motion as well as sudden displacements during earthquakes. GPS networks may be deployed in campaign (temporary) and permanent modes, but the decreasing cost and widespread use of this technology has been shifting more deployments to permanent status (Jordan, 2003). These data help in estimating earthquake potential, identifying active blind thrust faults and determining the potential response of major faults to the regional change in strain. As well, the ability of GPS technology to provide a measurement of the total slip caused by an earthquake complements traditional seismological methods of determining earthquake magnitude.

GPS measurements of crustal deformation are available for nearly all active tectonic environments. These data provide new and more accurate maps of the present crustal deformation field, a fundamental measurement of active continental tectonics. GPS data are important for studies of the earthquake source process since the measurement of surface displacement is mathematically related to a dislocation on a fault in an elastic medium. This relation permits the inversion of the geometry of the earthquake rupture. Such an inversion is more reliable when performed using near-field strong motion data (e.g., Bakun et al., 2005)

GPS data are also useful for the study of postseismic processes. The 1989 Loma Prieta, California, earthquake showed postseismic strain with a characteristic decay transient of 1.4 years (Savage et al., 1994). These authors report, contrary to expectations, that the transient parallel to the fault is smaller than the transient perpendicular to the fault. The interpretation of this observation is still debated.

GPS and older geodetic data have been used in a search for precursory crustal deformation prior to large earthquakes. Slow precursors were found for eight convergent margin earthquakes, including the 1960 9.2 M Chile, 1964 9.2 M Prince William Sound, Alaska, and the 1,700 Cascadian earthquakes (Roeloffs, 2006). On the other hand, no pre-seismic deformation was detected for the following terrestrial earthquakes: 2004 6.0 M Parkfield, 1992 7.3 M Landers, 2003 8.1 M

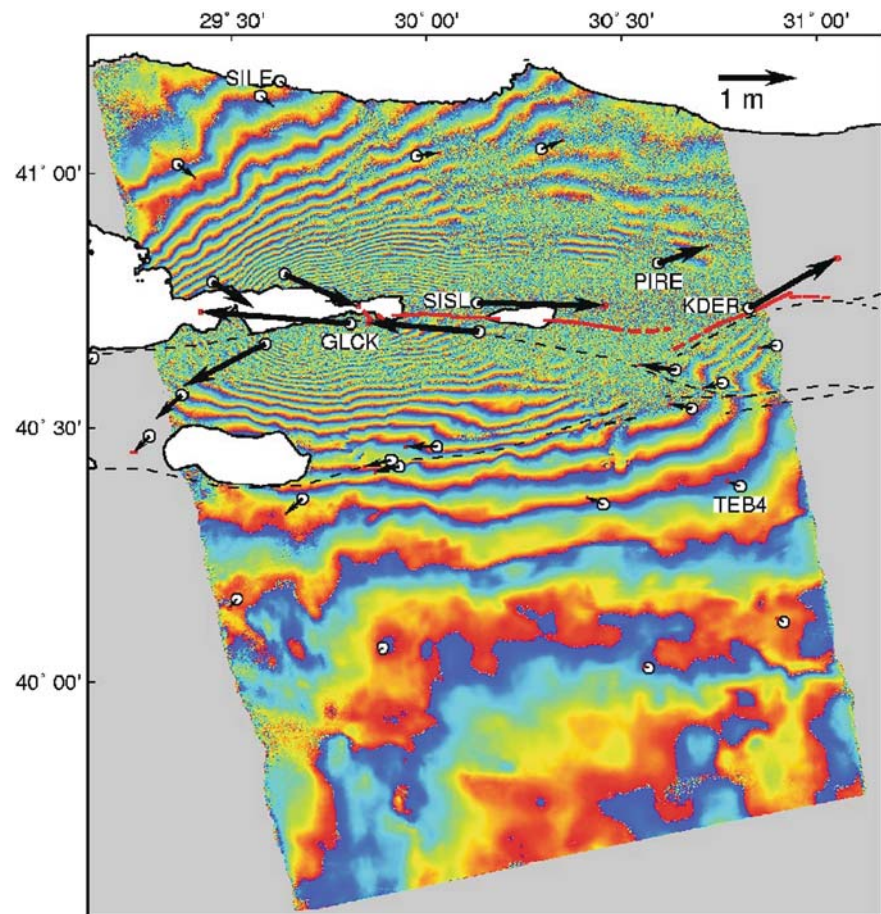
Tokachi-oki (Irwan et al., 2004), and 1999 7.1 M Hector Mine earthquakes (Mellors et al., 2002). Since slow creep can go entirely undetected unless high quality GPS array data are available, it is presently inconclusive how often earthquakes are preceded by slow aseismic slip. This is an important research topic.

Interferometric Synthetic Aperture Radar (InSAR)

InSAR is a recent, innovative technology that permits the imaging of earthquake (crustal) deformation down to the millimeter scale (Wright et al., 2001a). Similar to GPS measurements, radar waves are emitted from satellites across the globe to the Earth's surface. In the case of InSAR, these radio waves are reflected from the ground surface and returned to the satellite. The satellite is sensitive to both: (1) the intensity of the returning electromagnetic wave, which has a different signature depending on the nature of the ground material, and (2) the phase of the returning wave, which will have been altered if ground displacement has taken place between successive passes of the satellite over the same location. This technology opens the door to continuously mapping deformation along active plate boundaries over larger areas and in greater detail than can practically be monitored by GPS measurements. InSAR derived interferograms have successfully been used to acquire a rapid map of surface deformation after an earthquake, such as the 1999 Izmit earthquake and in tracking interseismic strain accumulation along a large section of the Northern Anatolian Fault through minute measurements of surface displacement over a nearly decadal timescale (Wright et al., 2001b; Fig. 13).

InSAR techniques are also effective in measuring deformation on active volcanoes and landslides, both of which are significant geological hazards. For example, magma movement can be detected at otherwise apparently dormant volcanoes. As more InSAR satellites come into orbit, the capability has emerged to make measurements more frequently, and thereby make greater use of the technique as a monitoring tool. InSAR measurements of fault slip complement determinations made using seismic and GPS measurements, and generally cover a wider geographic area.

Fig. 13 Radar interferogram for the Izmit earthquake (data copyright ESA) revealing the surface displacements, measured in the satellite's line-of-sight, in the 35-day period between the two image acquisitions. Each interference fringe is equivalent to 28 mm of displacement in the satellite line-of-sight, or approximately 70 mm if caused by pure horizontal motion. *Red lines* are the mapped surface rupture [Barka, 1999] and the *dashed lines* are previously mapped segments of the North Anatolian Fault [Şaroglu et al., 1992]. (after Wright et al., 2001a)



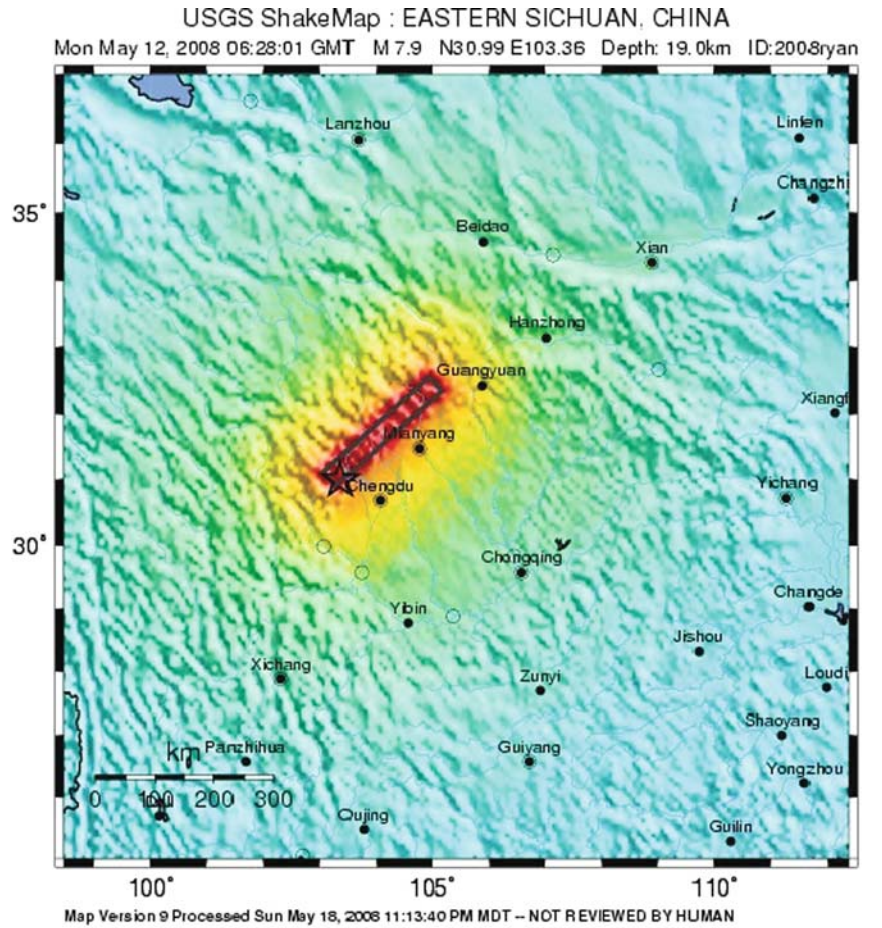
Shakemaps of Seismic Intensities

Seismic intensity is a measurement of the severity of an earthquake's effects at different sites. The Modified Mercalli Intensity (MMI) scale ranges from Roman numeral I to XII, the highest level being total destruction. The MMI scale predates instrumental recordings, and is derived from field observations of damage. The intensity for historical earthquakes can also be determined from newspaper accounts, diaries, and other documents. The local intensity of an earthquake is of greater importance than the earthquake magnitude to those who manage emergency response because the intensity directly relates to damage effects.

A recent key development by the U.S. Geological Survey and its partners is an online system that provides near-real-time post-earthquake information regarding ground shaking. Shakemap (Wald et al.,

2003) provides a map view of the ground shaking intensity in the region of an earthquake based on measurements from seismometers. Whereas an earthquake has a unique location and magnitude, the intensity of ground shaking it produces depends on such factors as the distance from earthquake, local site conditions and seismic wave propagation effects due to complexities in the structure of the Earth's crust. Shakemap software produces near real-time intensity maps for earthquakes, such as the May 12, 2008 Mw 7.9 Eastern Sichuan earthquake in China (Fig. 14). The widespread availability of such maps through the internet is valuable for the coordination of emergency response teams. The ground-shaking of hypothetical future earthquakes can also be evaluated, as well as the damage that would be associated with them today. ShakeMap thus serves as a useful, predictive tool by simulating the seismic intensity related to hypothetical future earthquakes.

Fig. 14 Seismic shaking intensity map produced by the USGS shortly after the Wenchuan, China. The map correctly indicated that a high population density NW of the epicenter were subjected to violent-to-extreme ground shaking intensities. Such maps, which are produced by processing data from local seismographs, are useful in planning earthquake emergency response



PERCEIVED SHAKING	Not felt	Weak	Light	Moderate	Strong	Very strong	Severe	Violent	Extreme
POTENTIAL DAMAGE	none	none	none	Very light	Light	Moderate	Moderate/Heavy	Heavy	Very Heavy
PEAK ACC.(%)	<.17	.17-1.4	1.4-3.9	3.9-9.2	9.2-18	18-34	34-65	65-124	>124
PEAK VEL.(cm/s)	<0.1	0.1-1.1	1.1-3.4	3.4-8.1	8.1-18	18-31	31-60	60-116	>116
INSTRUMENTAL INTENSITY	I	II-III	IV	V	VI	VII	VIII	IX	X+

Earthquake Forecasting vs. Earthquake Prediction

Earthquake *prediction* refers to the ability to calculate the specific magnitude, place and time for a particular future earthquake, similar to how meteorologists can now forecast an oncoming hurricane or tornado on a short timescale. The current state of earthquake science precludes any ability to truly predict specific future earthquakes. Earthquake *forecasting*, refers to modeling the probabilities that earthquakes of specified magnitudes, and faulting types will occur during a specified time interval (usually several years) on a specific

fault segment. Such probability estimates, when calculated over a specific time interval, are known as *time-dependent* earthquake forecasting. *Time-independent* forecasting, also known as long-term forecasting, is a general assessment of the likelihood of faults to rupture, not over a specific timeframe, and does not take into account whether earthquakes have occurred recently on particular faults. Time-independent forecasting is frequently used to evaluate building codes and developments or projects that must be sustainable in the long-term. A comparison between short-term and time-independent forecasting models can be found in Helmstetter et al. (2006). In order to calculate either type of earthquake probability forecast, a variety of

data are assembled and analyzed, including earthquake recurrence intervals from paleoseismic, historical and instrumental records, deformation and slip rates from GPS and InSAR and long-term plate-tectonic models.

In 2007, the Working Group on California Earthquake Probabilities (WGCEP) developed a state-wide rupture (time-dependent) forecast called the Uniform California Earthquake Rupture Forecast (UCERF). This probability map specifies the likelihood of a $M_w > 6.7$ earthquake striking California over the next 30 years (Field et al., 2008; Fig. 15). Such probability maps are critical to ensure public safety in regions of high seismic hazard such as California or Alaska. The UCERF forecast will be used by the

California Earthquake Authority (CEA) to analyze potential earthquake losses, set earthquake insurance premiums and develop new building codes.

Earthquake Early Warning

It is evident from the preceding review that much progress has been made in understanding earthquakes. Nevertheless, routine short-term earthquake prediction has not been achieved. Indeed, it will likely require many decades of additional research to address this problem. Therefore, it is useful to ask if it is feasible to provide an early warning of impending strong ground

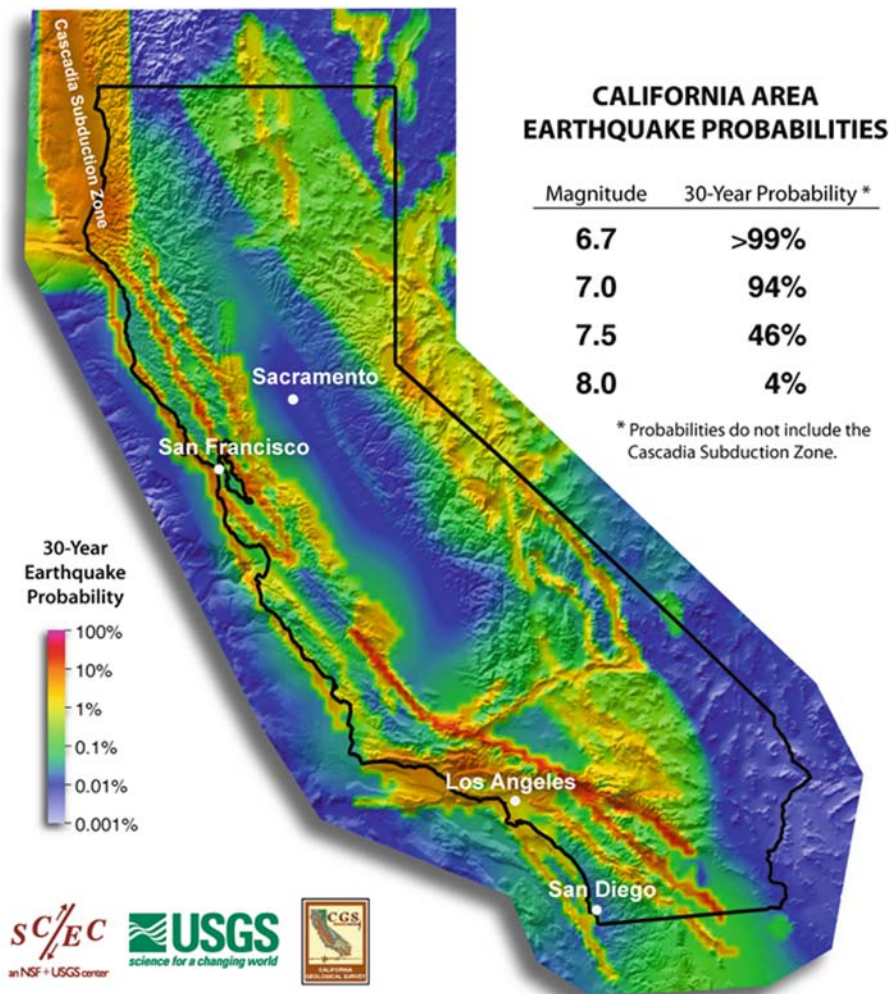


Fig. 15 Probabilistic earthquake hazard map for the State of California, USA, showing in yellow and orange those regions with higher probabilities for an earthquake with $M_w \geq 6.7$ in

the next 30 years. Boxes outlined in white located the Greater San Francisco and Greater Los Angeles areas with high seismic risk

motion based on an automated earthquake monitoring system, much as the lowered gates and flashing red lights at a railroad crossing announce the imminent arrival of a train.

Rapid earthquake notification is distinct from early warning systems. The former is a broadcast system that exists in many seismic networks that provides earthquake information within minutes after an earthquake occurs. In contrast, an early warning system provides an alert within seconds of the initial rupture of a significant ($M_w \geq 5$) earthquake, indicating that strong ground shaking can be expected. A warning that provides only some tens of seconds of advanced notice of incoming strong ground motion may appear inconsequential, but in fact it would allow enough warning time for critical systems (e.g., high-speed trains) to be shut down as well as for mobile individuals to take protective cover from falling objects. The physical basis for such a system, first realized by Cooper (1868), is the fact that electromagnetic signals (radio and internet communications) travel faster than elastic waves. Additionally, the first arriving P-waves have much lower ground motions than the later arriving surface waves.

Earthquake early warning systems need to estimate the potential magnitude of an earthquake within the first few seconds of the rupture process (Ellsworth and Beroza, 1995; Beroza and Ellsworth, 1996). The feasibility of such a system requires that there be sufficient information in the first-arriving compressional-wave (P-wave) at local seismic stations to estimate the potential size of the earthquake using empirical relations (Allen and Kanamori, 2003; Kanamori, 2005). Test cases show that there is a strong correlation between earthquake magnitude and the frequency content of the initial few seconds of the seismogram. Early warning systems use the information contained in the initial portions of the seismic waveforms (the P-wave arrival) to estimate the eventual magnitude of the earthquake. This method of waveform analysis, as well as other methods (Cua and Heaton, 2003), can provide robust earthquake early warnings, especially in densely instrumented regions, such as Japan, Taiwan, Europe, and California.

Earthquake early warning systems have already been successfully operated. Mexico successfully issued an early warning to the public with their Seismic Alert System (SAS) during the $M_w = 7.3$ September 14, 1995 Copala earthquake that occurred on the sub-

duction zone at the west coast, some 300 km from Mexico City. Over 4 million people in the city were warned. The success was in part due to the fact that the earthquake occurred during the day, when the majority of people were awake and had access to radios (Lee and Espinosa-Aranda, 1998). The Mexican Seismic Alert System consists of four units: seismic detection, telecommunications, central control, and early warning. The field stations are located 25 km apart, each monitor a region 100 km in diameter, and can estimate the magnitude of an earthquake within 10 s of its initiation. Other early warning systems have been installed in several other countries, including Japan, Taiwan, and Turkey (Lee et al., 1998). In view of the difficulty of achieving short-term earthquake predictions, earthquake early warning, like improved building codes, can be expected to play an increasingly important role in mitigating earthquake affects.

Closing Comments

Progress in the science of earthquakes, and the mitigation of earthquake effects has often been the results of knowledge gained from a devastating event. Examples include the earthquakes of 1906 in San Francisco, California; 1923 in the Kanto District, Japan; 1976 in Tangshan, China; and 2004 in Sumatra-Andaman Islands in Indonesia and India. We have highlighted some key concepts such as the earthquake cycle and recurrence intervals that are used in describing the underlying cause of earthquake. We have summarized some lessons learned from the earthquake record, such as the larger geographical area that experiences high seismic intensities for earthquakes that occur in continental interiors. Finally, we have described five important advances that have been made that have greatly enhanced our ability to monitor, report, and respond to large, damaging earthquakes. These five advances are: (1) enhanced seismic monitoring and notification; (2) GPS and (3) InSar monitoring; (4) the introduction of Shakemaps, and (5) progress in earthquake forecasting and early warning.

Have these steps succeeded in reducing earthquake hazards? The answer is certainly "Yes". Will these steps ensure a reduction in worldwide losses for the foreseeable future? The answer to this question is "Maybe". The reason for this equivocal answer is

multifold. As shown by the 2005 Kashmir, Pakistan, and 2008, Sichuan, China, earthquakes, rapid population growth is resulting in the urbanization of formerly remote, seismically hazardous regions. These two earthquakes were in relatively isolated mountainous regions, but both caused more than 70,000 deaths, with millions left homeless. Due to the mountainous topography, massive landslides and rock falls were an additional, secondary effect, in addition to the severe ground shaking. Secondary hazards pose a severe threat to all affected by an earthquake. The December 26, 2004 tsunami is a prime example; the tsunami wave was a secondary hazard produced by the $M_w = 9.2$ earthquake that occurred at the Sumatra subduction zone. Another example occurred in Chimbote, Peru in 1971, when a $M_w = 7.9$ earthquake struck off the coast of Peru, and a landslide buried the city of Yungay and thousands of its residents. These examples should serve as reminders that one should prepare not only for earthquake strong ground motion, but also its secondary repercussions for example.

Remote and mountainous regions are not the only population centers at heightened risk. The growth of the world's mega-cities also presents a great challenge. There are twenty-two cities that have a population greater than 10 million; the list of cities at risk from earthquakes includes: Tokyo, Lima, Los

Angeles, Mexico City, Beijing, Dhaka, Istanbul, Mumbai, Karachi, and Tehran. These ten cities comprise more than 120 million residents. Landslides and rock falls are not the main hazard in these megacities, building collapse and fires are. For this reason, the mitigation of earthquakes hazards in these cities depends on the adoption and enforcement of adequate building codes and fire safety. These new codes will require a very significant financial investment, one that in many cases may be beyond the reach of the local or national government.

Although some earthquakes have long recurrence intervals ($\geq 1,000$ years), they are still extremely dangerous – possibly even more than those with short recurrence intervals because these communities may fail to plan for earthquakes which they believe will not happen in their lifetime. Unfortunately, this was the case in the Sichuan province in China on May 12, 2008. The Longmen Shan fault system has a recurrence interval of about 2,000 years. As a result, the public was not prepared to deal with an earthquake of such great magnitude (Fig. 16).

Contrary to expectations, the death toll caused by an earthquake does not always correspond with the magnitude. Such was the case for the December 26, 2003 ($M_w = 6.6$) Bam, Iran earthquake that killed approximately 31,000 people, injured 30,000, and left 75,600

Fig. 16 Ruins of an ancient temple in Hanwang-Mianzhu, Sichuan, China. The destruction of the Wenchuan, China, earthquake reinforces the point that a long recurrence interval is not equivalent to safety. This temple withstood hundreds of years of environmental forces but was destroyed by the $M_w = 7.9$ earthquake on May 12, 2008. Source: Sarah Bahan, USGS



homeless. Some 85% of buildings in Bam were damaged or destroyed as a result of severe ground shaking, the main cause of damage to buildings and infrastructure. Furthermore, the proximity of a region to the seismic source is very important. The closer to the epicenter, the stronger the ground shaking will be.

Technological improvements hold the promise for reducing losses due to earthquakes. These improvements can be divided into two types: (1) better monitoring and risk assessment before an earthquake happens, and (2) improved reporting and response after the event occurs. Better seismic monitoring and GPS systems provide critical data for improved risk assessments. After an earthquake occurs, Shakemaps can be used to quickly and efficiently alert the government, media, and general public of the hazard. InSAR maps, if available quickly, provide a comprehensive picture of the region affected. Such technological advances will make it possible to continue to improve seismic hazard assessments, monitoring, mitigation and response.

References

- Allen R.M. and H. Kanamori, 2003, The potential for earthquake early warning in southern California. *Science* 300, 786–789.
- Bakun W, Aagaard B, Dost B, Ellsworth W, Hardbeck J, Harris R, Ji C, Johnston M, Langbein J, Lienkaemper J, Michael A, Nadeau R, Reasenburg P, Reichle M, Roeloffs E, Shakai A, Simpson R and Waldhauser F, 2005, Implications for prediction and hazard assessment from the 2004 Parkfield earthquake. *Nature* V. 437, p. 969–974.
- Barka A., 1999, The 17 August 1999 Izmit earthquake. *Science* 285, 1858–1859.
- Belardinelli M.E., Bizzarri A., Cocco M., 2000, Earthquake triggering by static and dynamic stress changes. *Eos Trans. AGU*, Fall Meet. Suppl, 81, 48.
- Beroza G.C. and W.L. Ellsworth, 1996, Properties of the seismic nucleation phase. *Tectonophysics* 261, 209–227.
- Bolt B., 2006, *Earthquakes*. Fifth edition. W. H. Freeman and Company, New York.
- Brace W., and Kohlstedt D., 1980, Limits on lithospheric stress imposed by laboratory measurements. *J. Geophys. Res.* 85, 6248–6252.
- Burchfiel B.C., Z. Chen, Y. Liu, L.H. Royden, 1995, *Tectonics of the Longmen Shan and adjacent regions, central China*. *Int. Geol. Rev.* 37, 8, edited by W.G. Ernst, B.J. Skinner, L.A. Taylor.
- Calais E., Han J.Y., DeMets C., d Nocquet J.M., 2006, Deformation of the North American plate interior from a decade of continuous GPS measurements. *J. Geophys. Res.* 111, doi: 10.1029/2005JB004253.
- Campbell D.L., 1978. Investigation of the stress-concentration mechanism for intraplate earthquakes, *Geophys. Res. Lett.*, 5(6), 477–479.
- Chandrasekhar D.V. and Mishra D.C., 2002. Some geodynamic aspects of Kutch basin and seismicity: An insight from gravity studies, *Curr. Sci. India*, 83(4), 492–498.
- Cloetingh S., 1982. Evolution of passive margins and initiation of subduction zones, Ph.D. thesis, Utrecht Univ., Netherlands.
- Cooper J.D., 1998. Letter to the Editor, San Francisco Daily Evening Bulletin, Nov. 3, 1868 (as quoted in Lee and Espinosa-Aranda, 1998).
- Cua G. and T.H. Heaton, 2003. An envelope-based paradigm for seismic early warning, (abstract) *Trans. Am. Geophys. Union* 84, F1094–1095
- Cutcliffe C. H. 2000. Earthquake resistant building design codes and safety standards: The California experience. *Geophys. J.*, 51, 259–262.
- Dragert H. and Hyndman R., 1995. Continuous GPS monitoring of elastic strain in the northern Cascadia subduction zone. *Geophys. Res. Lett.* 22:755–758.
- Dragert H; Wang K; James TS, 2001. A Silent Slip Event on the Deeper Cascadia Subduction Interface. *Science* 292(5521): 1525–1528.
- Ellsworth W.L. and G.C. Beroza, 1995. Seismic evidence for an earthquake nucleation phase. *Science* 268, 851–855.
- Eshghi S. and Zaré M. 2004. Preliminary observations on the Bam, Iran, earthquake of December 26, 2003. *EERI Special Earthquake Report*.
- Field E.H., Dawson T.E., Felzer K.R., Frankel A.D., Gupta V., Jordan T.H., Parsons T., Petersen M.D., Stein R.S., Weldon II R.J., Wills C.J., 2008. The Uniform California Earthquake Rupture Forecast, Version 2 (UCERF 2), U.S. Geological Survey Open-File Report 2007-1337, CGS Special Report 203, SCEC Contribution #1138.
- Frankel A., Mueller C., Barnhard T., Perkins D., Leyendecker E., Dickman N., Hanson S., Hopper M., 1996. National Seismic Hazard Maps: Documentation June 1996, U.S. Geological Survey Open-File Report 96-532, Denver, CO, 111 pp.
- Freed A.A., 2005, Earthquake triggering by static, dynamic, and postseismic stress transfer, *Ann. Rev. Earth Planet. Sci.*, 33, 335–367.
- Freed A. M., Ali S. T. and Burgmann R. 2007. Evolution of stress in Southern California for the past 200 years from coseismic, postseismic and interseismic stress changes. *Geophys. J. Int.*, 169, 1164–1179.
- Gangopadhyay A. and Talwani P., 2003. Symptomatic features of intraplate earthquakes, *Seism. Res. Lett.*, 74, 863–883.
- Goetze C., 1978. The mechanisms of creep in olivine, *Phil. Trans. Roy. Soc. Lond. A.*, 288, 99–119.
- Goodacre A.K. and Hasegawa H.S., 1980. Gravitationally induced stresses at structural boundaries, *Can. J. Earth Sci.*, 17, 1286–1291.
- Gordon R.G., 1995. Plate motions, crustal and lithospheric mobility, and paleomagnetism: prospective viewpoint. *J. Geophys. Res.*, v. 100, p. 24367–24392.
- Gordon R.G. and Stein S., 1992. Global tectonics and space geodesy. *Science*, v. 256, p. 333–342.
- Gupta H.K., Rastogi B.K., and Narain H., 1972, Common features of the reservoir-associated seismic activities, *Bull. Seis. Soc. Am.*, 62, 481–492.

- Grollmund B. and Zoback M.D., 2001. Did deglaciation trigger intraplate seismicity in the New Madrid seismic zone?, *Geology*, 29(2), 175–178.
- Helmstetter A., Kagan Y.Y., and Jackson D.D., 2006. Comparison of Short-Term and Time-Independent Earthquake Forecast Models in Southern California. *Bull. Seismol. Soc. Am.*, v. 96, no. 1, p. 90–106.
- Hinze W.J. et al., 1988. Models for Midcontinent tectonism: an update, *Rev. Geophys.*, 26(4), 699–717.
- Hirose H., et al. 1999. A slow thrust slip event following the two 1996 Hyuganada earthquakes beneath the Bungo Channel, southwest Japan. *Geophys. Res. Lett.* 26(21): 3237–3240.
- Irwan M., Kimata F., Hirahara K., Sagiya T., Yamagiwa A., 2004. Measuring ground deformations with 1-Hz GPS data: the 2003 Tokachi-oki earthquake (preliminary report). *Earth Planets Space*, 56: 389–393. http://news.thomsonet.com/IMT/archives/2007/07/earthquake_japan_nuclear_kashiwazaki-kariwa_plant_industry_automotive_production_halt.html
- Johanson I.A., Fielding E.J., Rolandone F., and Buergermann R., 2006. Coseismic and postseismic slip of the 2004 Parkfield earthquake from space-geodetic data. *Bull. Seismol. Soc. Am.*, 96(4B):S269–S282.
- Johnston A.C. and Kanter L.R., 1990. Earthquakes in stable continental crust, *Sci. Am.*, 262(3), 68–75.
- Johnston A. C., Coppersmith K. J., Kanter L.R. and Cornell C.A., 1994. The earthquakes of stable continental regions: assessment of large earthquake potential, TR-102261, Vol. 1–5, ed. Schneider J.F., *Electric Power Research Institute (EPRI)*, Palo Alto, CA.
- Jordan T. 2003. *Living on an Active Earth: Perspectives on Earthquake Science*. The National Academies Press: Washington, D.C.
- Kanamori H., (2005). Real-time seismology and earthquake damage mitigation. *Ann. Rev. Earth Planet. Sci.* 33, 195–214.
- Kayal J.R., Zhao D., Mishra O.P., De R., Singh O.P., 2002, The 2001 Bhuj earthquake: Tomographic evidence for fluids at the hypocenter and its implications for rupture nucleation, *Geophys. Res. Lett.*, 29, 2152–2155.
- Kenner S.J. and Segall P., 2000. A mechanical model for intraplate earthquakes; application to the New Madrid seismic zone, *Science*, 289(5488), 2329–2332.
- King G.C.P., Stein R.S. and Lin J., 1994, Static stress changes and the triggering of earthquakes, *Bull. Seismol. Soc. Am.*, 84, 935–953.
- Kostoglodov V., et al., 2003. A large silent earthquake in the Guerrero seismic gap, *Mexico. Geophys. Res. Lett. Col.* 32(15): 1807, doi:10.1029/2003GL017219.
- Lawson A.C. (Ed.), 1908, *The California earthquake of April 18, 1906*. Report of the State Earthquake Investigation Commission. (reprinted in 1969 by the Carnegie Institution of Washington, D.C.).
- Lee W. H. K. and Espinosa-Aranda J. M., 1998. Earthquake Early Warning Systems: Current Status and Perspectives in Early Warning Systems for Natural Disaster Reduction. J. Zschau and A. N. Koppers, Eds. Springer, New York: 834 pp.
- Lee W.H.K. and Espinosa-Aranda J.M., 2003. Earthquake early warning systems: Current status and perspectives: in 'Early Warning Systems for Natural Disaster Reduction', J. Zschau and A. N. Koppers, Eds. Springer, Berlin: pp. 409–423.
- Liu L. and Zoback M.D., 1997. Lithospheric strength and intraplate seismicity in the New Madrid seismic zone, *Tectonics*, 16(4), 585–595.
- Long L.T., 1988. A model for major intraplate continental earthquakes, *Seism. Res. Lett.*, 59(4), 273–278.
- Lowry AR; Larson KM; Kostoglodov V; Bilham R. Transient fault slip in Guerrero, southern Mexico. *Geophys. Res. Lett.*, vol. 28, no.19, pp. 3753–3756, 2001.
- Mandal P., and Rastogi B.K., 2005, Self-organized fractal seismicity and b value of aftershocks of the 2001 Bhuj earthquake in Kutch (India): *Pure Appl. Geophys.*, v. 162, no. 1, p. 53–72.
- Melbourne TI, and FH Webb., 2003, Slow but not quite silent. *Science* 300: 1886–1887.
- Mellors R.J., Sichoix L., Sandwell D.T., 2002. Lack of precursory slip to the 1999 Hecot Mine, California, earthquake as constrained by InSAR. *Bull. Seis. Soc. Am.* 92: 1443–1449.
- Mishra O.P. and ZhaoD., 2003, Crack density, saturation rate and porosity at the 2001 Bhuj, India, earthquake hypocenter: a fluid-driven earthquake?, *Earth Planet. Sci. Lett.*, 212 (3–4), 393–405.
- Mohindra R. and Bagati T.N., 1996, Seismically induced soft-sediment deformation structures (seismites) around Sumdo in the lower Spiti valley (Tethys Himalaya), *Sediment. Geol.*, 101, 69–83.
- Murray J. and Langbein J., 2006. Slip on the San Andreas Fault at Parkfield, California, over two earthquake cycles, and the implications for seismic hazard. *Bull. Seismol. Soc. Am.*, 96(4B):S283–S303.
- Naseem A., Ali Q., Javed M., Hussain Z., Naseer A., Ali S. M., Ahmed I., Ashraf M., Scawthorn C. 2005. First report on the Kashmir earthquake of October 8, 2005. *EERI Special Earthquake Report*.
- Nelson A.R., Atwater B.F., Bobrowsky P.T., Bradley L.A., Clague J.J., et al., 1995. Radiocarbon evidence for extensive plate-boundary rupture about 300 years ago at the Cascadian subduction zone. *Nature* 378: 371–374.
- Quinlan G., 1984. Postglacial rebound and the focal mechanisms of eastern Canadian earthquakes, *Can. J. Earth Sci.*, 21, 1018–1023.
- Raphael A., and Bodin P., 2002, Relocating aftershocks of the 26 January 2001 Bhuj earthquake in western India. *Seis. Res. Lett.* 73, 417–418
- Reid H.F., 1910, *The Mechanics of the Earthquake*, The California Earthquake of April 18, 1906, Report of the State Investigation Commission, Vol.2, Carnegie Institution of Washington, Washington, D.C.
- Roeloffs E, May 2006, Evidence for Aseismic Deformation Rate Changes Prior to Earthquakes. *Annual Review of Earth and Planetary Sciences*. Vol. 34: 591–627. (doi:10.1146/annurev.earth.34.031405.124947)
- Rogers G., and Dragert H., 2003. Episodic Tremor and Slip on the Cascadia Subduction Zone: The Chatter of Silent Slip. *Science* 300(5627): 1942–1943.
- Şaroglu F., Ö. Emre, and I. Kuşçu, Active Fault Map of Turkey, General Directorate of Mineral Research and Exploration (MTA), Eskişehir Yolu, 06520, Ankara, Turkey, 1992.
- Satake K. and Atwater B.F., 2007. Long-Term Perspectives on Giant Earthquakes and Tsunamis at Subduction Zones. *Annu. Rev. Earth Planet. Sci.* 35:349–374.

- Savage J.C., Lisowski M., Prescott W.H., 1981. Geodetic strain measurements in Washington. *J. Geophys. Res.* 86: 4929–4940.
- Savage J.C., Lisowski M., Svarc J., 1994. Postseismic deformation following the 1989 ($M = 7.1$) Loma Prieta, California, earthquake. *J. Geophys. Res.*, 99, 13757–13765.
- Sbar M.L. and Sykes L.R., 1973. Contemporary compressive stress and seismicity in eastern North America: An example of intra-plate tectonics, *Geol. Soc. Am. Bull.*, 84, 1861–1882.
- Schulte S.M. and Mooney W.D., 2005. An updated global earthquake catalogue for stable continental regions: reassessing the correlation with ancient rifts. *Geophys. J. Int.* 161, 707–721.
- Segall P. and Davis J.L., 1997. GPS applications for geodynamics and earthquake studies, *Ann Rev. Earth Planet. Sci.*, 25, 301–336.
- Shishikura M., 2003. Cycle of interpolate earthquakes along the Sagami Trough deduced from tectonic geomorphology, *Bull. Earthquake Res. Inst. Univ. Tokyo* 78, 245–254.
- Simpson D.W., 1986. Triggered earthquakes, *Ann. Rev. Earth Planet. Sci.*, 14, 21–42.
- Sokoutis D. et al. Insights from scaled analogue modeling into the seismotectonics of the Iranian region. *Tectonophysics* Volume 376, Issues 3–4, 4 December 2003, pp. 137–149
- Stein R.S., Barka A.A., and Dieterich J.H., 1997. Progressive failure on the North Anatolian fault since 1939 by earthquake stress triggering, *Geophys. J. Int.*, 128, pp. 594–604.
- Stein R.S., 1999. The role of stress transfer in earthquake occurrences, *Nature* 402, 605–609.
- Stein R.S., Toda S., Parsons T. And Grunewald E., 2006. A new probabilistic seismic hazard assessment for greater Tokyo, *Phil. Trans. R. Soc. A*, 1965–1988, doi:10.1098/rsta.2006.1808.
- Stein S., Sleep N., Geller R.J., Wang S.C. and Kroeger G.C., 1979. Earthquakes along the passive margin of eastern Canada, *Geophys. Res. Lett.*, 6(7), 537–540.
- Sykes L.R., 1978. Intraplate seismicity, reactivation of preexisting zones of weakness, alkaline magmatism, and other tectonism postdating continental fragmentation, *Rev. Geophys.*, 16(4), 621–688.
- Tagare G. V. 2002. Earthquakes: Some ancient speculations. Speech given at the Institute for Oriental Study, Thane, India. <http://www.orientalthane.com/speeches/gvtagare/1.html>
- Talwani P., 1988. The intersection model for intraplate earthquakes, *Seism. Res. Lett.*, 59(4), 305–310.
- Talwani P., 1999. Fault geometry and earthquakes in continental interiors, *Tectonophysics*, 305, 371–379.
- Talwani P. and Rajendran K., 1991. Some seismological and geometric features of intraplate earthquakes, *Tectonophysics*, 186, 19–41.
- Tuttle M.P., Schweig III, E.S., Campbell J., Thomas P.M., Sims J.D., Jafferty III, R.H., 2005. Evidence for New Madrid earthquakes in
- United Nations Population Division. World population prospects: the 2002 Revision. <http://www.un.org/popin/data.html>
- USGS Earthquake Hazard Summary, Magnitude 8.0 – NEAR THE COAST OF CENTRAL PERU, 2007. <http://earthquake.usgs.gov/eqcenter/eqinthenews/2007/us2007gbcv/#summary>
- USGS earthquake summary for the July 16, 2007 earthquake in Japan. <http://earthquake.usgs.gov/eqcenter/eqinthenews/2007/us2007ewac/>
- Vinnik L.P., 1989. The origin of strong intraplate earthquakes, translated from O prirode sil'nykh vnutrilplitovykh zemlyasenyi, *Doklady Akademii Nauk SSSR*, 309(4), 824–827.
- Wald D., Wald L., Worden B., and Goltz J., 2003. ShakeMap – A tool for earthquake response, US Geological Survey Fact Sheet FS-087-03. (available at: <http://pubs.usgs.gov/fs/fs-087-03/>)
- West M., Sanches J.J., McNutt S.R., 2005. Periodically Triggered Seismicity at Mount Wrangell, Alaska, After the Sumatra Earthquake. *Science* Vol. 308, No. 5725, 1144–1146.
- Wright T.J., E.J. Fielding and B.E. Parsons, 2001a. Triggered slip: observations of the 17 August 1999 Izmit (Turkey) earthquake using radar interferometry, *Geophys. Res. Lett.*, 28(6), 1079–1082.
- Wright T.J., Parsons B.E. Fielding E.J., 2001b. Measurement of interseismic strain accumulation across the North Anatolian Fault by satellite radar interferometry, *Geophys. Res. Lett.* 28(10), 2117–2120.
- Xu X., Yu G., Klinger Y., Tapponnier P. & Van Der Woerd J., 2006. Reevaluation of surface ruion of the 2001 Kunlunshan earthquake ($M_w 7.8$), northern Tibetan Plateau, China, *J. Geophys. Res.*, 111, B05316, doi:10.1029/2004JB003488.
- Zoback M.L. and Zoback M.D., 1980. State of stress in the conterminous United States, *J. Geophys. Res.*, 85, 6113–6156.
- Zoback M.D., 1983. Intraplate earthquakes, crustal deformation and in-situ stress, in *A workshop on 'The 1886 Charleston, South Carolina, earthquake and its implications for today'*, Open-File Report, No. 83–843, pp. 169–178, eds Hays, W.W., Gori, P.L. and Kitzmiller, C., US Geological Survey, Reston, VA.
- Zoback M.D. and Townend J., 2001. Implications of hydrostatic pore pressure and high crustal strength for the deformation of intraplate lithosphere, *Tectonophysics* 336, 19–30.
- Zoback M.L., 1992. First- and second-order patterns of stress in the lithosphere: the world stress map project. *J. Geophys. Res.*, 97, 11703–11728
- Zoback M.L. and Richardson R.M., 1996. Stress perturbation associated with the Amazonas and other ancient continental rifts, *J. Geophys. Res. B Solid Earth Planets*, 101(3), 5459–5475.